AIAA 80-0689R

Postbuckling Behavior of Composite Shear Webs

B. L. Agarwal*
Northrop Corporation, Hawthorne, Calif.

In this paper the postbuckling behavior of multibay composite shear webs is explored. Several test specimens are designed through the use of advanced state of the art design methods taking into account material anisotropy. The panels are subjected to static as well as fatigue loading in a series of well instrumented and carefully conducted tests to determine various failure modes as well as failure loads. The experimentally observed failure modes and failure loads are compared with design loads and failure modes. Large deflection analysis is used to examine failure modes typical of composite panels. Composite shear webs are shown to have significant postbuckling strength and exhibit failure modes that are quite different from metal shear webs.

Introduction

STRINGER-STIFFENED shear panels are used extensively in many metal aircraft applications. In many of these applications buckling of the skin between the stringers is permitted to occur below limit load—sometimes well below. Composite materials are undergoing a rapid use escalation in new and projected systems. In order to make composite components weight efficient as well as cost competitive with their metal counterparts, the postbuckling strength of composite materials must be exploited. The available data in the literature indicate that composite materials have significant postbuckling strength. Postbuckling strength of boron-epoxy shear webs is demonstrated by Kaminski and Ashton.[1] In a similar study by Bhatia,[2] graphite-epoxy shear webs are shown to have considerable postbuckling strength.

In metal structures, the principal structural concern for postbuckled shear webs is that significant permanent set not occur for loading up to limit loads. Fatigue and "wear out" are not of concern. For advanced composite stiffened panels, the concern about postbuckling behavior is much greater. Catastrophic failure can occur in the buckled skin due to high local compressive stresses or tension stresses; the relieving effects of yielding, as found in most metal structures, are not available in most practical composite layups. These compressive stresses, in addition to tension stresses present in shear webs, may result in severe strength degradation of composite laminates when subjected to repeated fatigue cycles. The purpose of this paper is to evaluate the behavior of realistically configured multibay panels operating well into the postbuckled regime, to disclose specific failure modes, to assess the adequacy (or inadequacy) of available buckling and strength prediction methodology, to provide direction for future research, and to provide confidence in the viability of this useful type of construction.

The main components of a shear beam are the web, uprights, and chords. The web transfers and/or resists the applied shear. The uprights are used to increase the buckling load of the web and to resist compression loads that are introduced from the tendency of the tension field forces in the web to pull the chords together. The chords together with the uprights prevent the structure from collapsing and are subjected to primary axial compression and tension loads due to primary bending of the beam as well as to secondary bending about their own axes due to the vertical component of the diagonal tension field forces. In metal shear beams, all three components can be designed separately with sufficient accuracy based upon what is generally referred to as "tension field theory." The theory has been developed for metals and is semiempirical in nature. The theory of pure diagonal tension was first developed by Wagner[3] and is not applicable to webs subjected to maximum loads that are of the order of the initial buckling load. The theory was extended to account for partial tension field action and to account for other modes of failure by Kuhn et al.,[4] Tsongas and Ratay,[5] and Darevics and Hoy[6] based upon the results of several hundred tests.

A theory for the design and analysis of composite shear beams does not exist at present. Some researchers have proposed the use of existing metal theory for composite webs as a first step. Although this may seem to be logical, there are several "fear factors" and unknowns that have to be overcome before such a theory can be used with any degree of confidence. Composite materials are nonhomogeneous and brittle, and hence exhibit several modes of failure which are quite different from those exhibited by metals. The theory developed for metals has been established principally for aluminum, and there is no evidence that the theory will apply equally to composites. The modes of failure that are considerably different in composites than in metals are web delamination, compression failure of the web, and debonding of the stiffeners from the web.

There have been some attempts to predict the behavior of shear beams by more refined analytical methods. The main difficulty in developing an accurate analysis method is that the postbuckling behavior of webs results in nonlinear equations that cannot be solved analytically. Several large scale computer codes that have a nonlinear capability, such as STAGS,[7] ANSYS,[8] and NASTRAN,[9] are available. However, the main difficulty in determining the strength of a composite shear web through the use of these analysis techniques arises from the lack of a suitable failure criterion. Although the basic strains and stresses at a given load level can be calculated, they can not be related generally to failure for all the different modes of failure. In the absence of a general failure criterion, the prediction of shear web laminate strength is dependent heavily on experimental data.

Selection of Test Fixture

The selection of a suitable test fixture for shear web testing is a nontrivial job. Several test fixtures have been used over the years for this purpose. The choice of the test fixture for the present program was made based upon the efficiency and the effectiveness of the test fixture, as well as on its adaptability to changes in web configuration without major modifications. The various candidate test fixtures are now reviewed.

Presented as Paper 80-0689 at the AIAA/ASME/ASCE/AHS 21st Structures, Structural Dynamics and Materials Conference, Seattle, Wash., May 12-14, 1980; submitted June 19, 1980; revision received Jan. 19, 1981.

*Engineering Specialist, Structural Mechanics Department, Aircraft Division. Member AIAA.

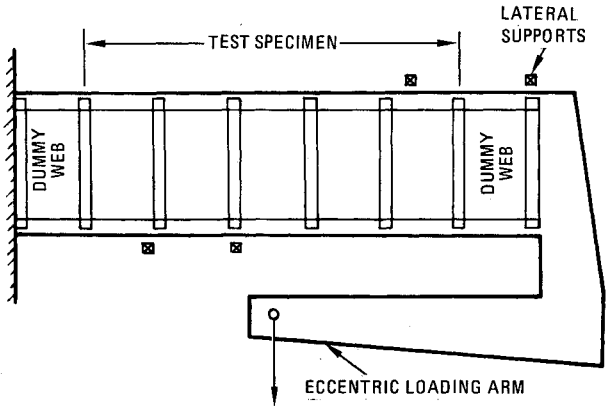

Fig. 1 Cantilever beam with eccentric loading arm.

Table 1 Test specimen matrix

Panel number	Stiffener configuration	Dimension D (cm)[a]	Dimension L (cm)[a]	Loading
1A	Hat	33.0	101.6	Static
1B	Hat	33.0	101.6	Fatigue
2A	I	33.0	101.6	Static
2B	I	33.0	101.6	Fatigue
3A	Hat	22.86	63.5	Static
3B	Hat	22.86	63.5	Fatigue

[a] Dimensions D and L are shown in Fig. 2.

The simplest and most economical fixture, used for the testing of unstiffened shear webs, is the "picture frame." The main advantages of this type of fixture are convenience and economy. The specimen is simple, and test set-up time is quite short. However, the fixture produces severe tension and compression strain concentrations at the corners. A strain concentration greater than 70% was measured for an unstiffened graphite-epoxy shear web.[10] Various methods, such as diagonal slots or cutouts at the corners, have been employed to reduce this concentration, but with limited success. In any event, the fixture is unsatisfactory for stiffened shear webs because the heavy edge members preclude any appreciable compression load on the uprights.

A short beam specimen loaded at each end by eccentric loading arms is used by Melvin.[11] In this setup, dummy bays are provided to prevent undue strain concentrations at the corners of the test bay by providing web continuity. They also serve to introduce the shear into the test web uniformly. This fixture has reduced chord loads and also has the advantages of a simple specimen and short test set-up time. The disadvantage is that the energy released at failure of the test web may deform the chords to a degree requiring replacement. Although this fixture is a substantial improvement over the picture frame for unstiffened web tests, the single test bay precludes realistic loading of the uprights.

Most of the metal tension field beam tests conducted in the past had cantilever beam specimens. The cantilever beam specimen has the advantage of accurately simulating the response of actual aircraft structure with one exception. A difficulty arises in testing due to lateral instability of the compression chord. The usual solutions are to increase the size of the chord and to add lateral supports. In an actual tension field beam, deflection of the chords between the uprights causes a shear concentration in the corners. This concentration is a "real-life" effect, and must be evaluated by test. Increasing the size of the chords tends to obscure this effect. The other solution, lateral supports, complicates the test setup and increases the expense. A second difficulty with cantilever beams is the result of less than infinite rigidity of the support. Even slight rotation of the support complicates determination of the beam stiffness. Simply supported beams

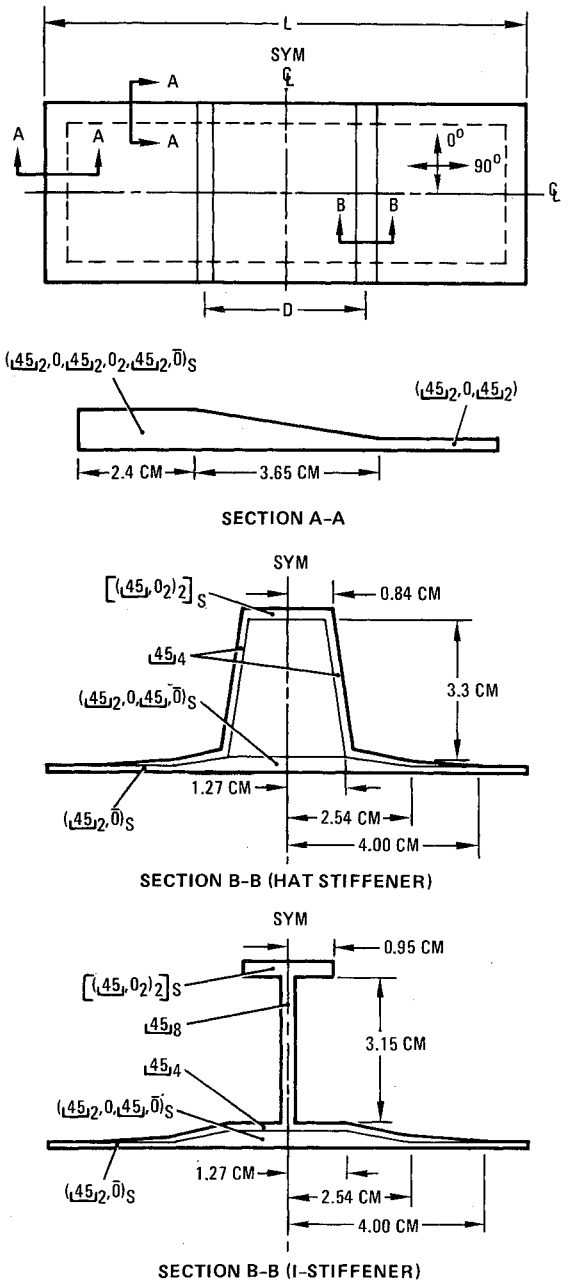

Fig. 2 Panel and stiffener details.

have been used to eliminate this difficulty through the use of a reinforced center bay. Reinforcing the center bay means each half of the simple beam must be twice as long as an equivalent cantilever beam to reproduce the upright loads as accurately as the cantilever beam. This increase in length greatly increases the lateral stability problem and substantially increases the cost of the specimen.

Tsongas and Ratay[5] and Darevics and Hoy[6] very successfully used a cantilever beam with an eccentric loading arm at the free end. This arrangement is a compromise between a cantilever beam specimen and the eccentrically loaded short beam specimen as illustrated in Fig. 1. With this configuration, realistic chord areas are possible due to the reduced chord loads. However, some degree of lateral support may still be required. A test setup similar to the one shown in Fig. 1 is used in the present experiments.

The test panel is attached to the fixture by 0.634-cm bolts at approximately 2.54-cm spacing along all four edges. The end bays have 0.634-cm aluminum plates as webs to allow the shear load to be transferred to the test panels. The caps (chords) in the test fixture are steel and are quite stiff.

Test Specimens

The specimen configuration selected for this program consists of a stiffened panel with two cocured stiffeners. The panel edges are increased in thickness to allow for the load from the test fixture to be introduced into the panel without failure. The panel stiffeners are quite stiff to assure that the failure occurs in the panel skin. The skin of the panel is allowed to buckle at about 17.5 kN/m of shear load which is a typical shear loading for a V/STOL fuselage panel in level flight.

Six specimens are fabricated and tested in accordance with the test matrix shown in Table 1. Identical panels A and B are subjected to static and fatigue load, respectively. Two different stiffener spacings are used to obtain different initial buckling loads. The stiffener shape for specimens 2A and 2B is an I section as opposed to the hat section for panels 1A and 1B to explore the differences in the behavior of open sections and closed sections, respectively. The sectional properties are kept identical except for the torsional stiffness. The basic details of the test specimen are shown in Fig. 2. The main material used for the fabrication of these panels is 3501-5 HMF 133 woven graphite-epoxy, and 3501-6/AS graphite epoxy tape material is used as needed. The symbol □ is used in Fig. 2 for woven material.

The panels are fabricated using removable rubber mandrels. The stiffeners are cocured with the skin. For the hat-stiffened panels, the stiffeners are laid over the rubber mandrel, and then a vacuum bag is used to keep the stiffener shape. For the I-stiffened panels, rubber mandrels are used on both sides of the vertical leg, and then the whole assembly is vacuum bagged and cured.

Test Procedures

The static load is applied with a hydraulic cylinder. The pressure to the cylinder is controlled with an Edison hydraulic proportioning unit to maintain fine control. The load is measured by a load cell, and strain data are recorded at each load increment.

The fatigue loading is applied with a hydraulic actuator controlled by a servo valve with a load cell mounted in series. A servo controller driven by a frequency generator provides the signal to the servo valve and accepts feedback signals from the load cell. The control unit includes a cycle counter that is preset to stop testing at the required number of cycles. Specimen protection from overloading is provided by a relief valve set to relieve at slightly above the programmed maximum load. The foregoing loading mechanism is load controlled.

Strain gages and dial gages are used to measure the experimental behavior of the test panel. Panel 1A is instrumented extensively to evaluate the test fixture as well as to provide guidelines for the instrumentation of the remaining panels. Ten back-to-back rosettes and 18 axial gages are used to measure strain, and 11 deflection gages are used to measure deflection at several locations on the shear web and on the metal chord. The remaining panels are instrumented with 4 rosettes and 4 axial gages. Back-to-back rosettes are used to determine the onset of buckling and the strain in the stiffeners.

Six panels with characteristics of stiffeners, geometry, and loading are listed in Table 1. None of the panel tests are replicated. The panels tested statically are first loaded in small increments to determine the onset of buckling load and then loaded slowly to failure. The fatigue panels are first loaded to the maximum fatigue load amplitude in a manner similar to the static test panels. The load amplitude is determined by taking approximately ⅔ of the static ultimate failure load for the corresponding test panels. The panels are then subjected to 500,000 cycles of constant amplitude fatigue loading ($R = 1$) at a loading rate of 2 Hz. At the end of the fatigue loading, the panel residual strength is measured. Strains are measured for each of the panels during every static load increment. Some of the panels are also equipped with a Moire grid to observe the normal deflection contours visually. However, no quantitative measurements are made using the Moire grid.

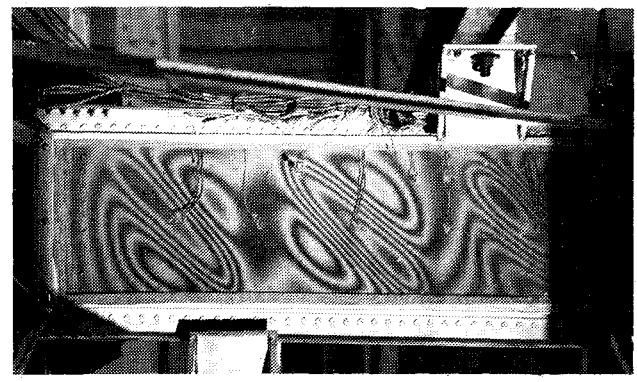

Fig. 3 Moire fringes of the panel at failure.

Test Results

Test panel 1A is loaded statically to a failure load of 177 kN/m. A loud noise is heard at this load level, and a crack is clearly visible in the diagonal tension corner due to bending caused by the buckles. The crack along with Moire fringes at failure is shown in Fig. 3. The buckling load of the center bay, as indicated by modified Southwell's method, is calculated to be 17.5 kN/m. The end bays are found to buckle soon after the center bay at a load of 23.3 kN/m. The panel ultimate failure load is about ten times the initial buckling load; thus, a considerable amount of postbuckling strength exists. The strains measured in the direction of tension fields vary almost linearly with the load. The strain measurements show considerable strain concentrations normal to the direction of tension fields caused by the buckles. Thus, a very high compressive strain results on one of the web surfaces. The measured maximum strain values at failure correspond quite well to the material allowables, as will be discussed later. The deflection gages located along the chord indicate no bending of the chord due to tension fields.

Panel 1B, which is identical to panel 1A, is subjected to constant amplitude fatigue loading with a maximum load amplitude of 105 kN/m. A delamination of a stiffener from the web is noted in one of the tension field corners after 20,000 cycles. This delamination is about 5 cm in size. A similar delamination appears in the diagonally opposite corner soon after the first delamination. These delaminations grow in size as additional fatigue cycles are applied. However, the growth of these delaminations stops at the end of approximately 50,000 cycles of fatigue loading. The fatigue loading is continued to a total of 500,000 cycles. The panel when tested for residual strength fails at a load of 185 kN/m. The failure is quite catastrophic resulting in severe damage to the panel as well as the test fixture. The strain gage data indicates the onset of initial buckling load to be 18.7 and 5.85 kN/m before and after fatigue loading, respectively. Thus, a considerable reduction in the initial buckling load is caused by fatigue. This reduction in buckling load is found to have no effect on the panel ultimate strength. The strains in the panel at various locations after fatigue loadings are found to be about 10% higher than the strains before fatigue, as shown in Fig. 4. Thus, there is some degradation in the panel stiffness, probably due to the delamination of stiffener from the skin.

Test panels 2A and 2B with I-section stiffeners are found to behave quite similarly to their counterpart panels 1A and 1B with hat stiffeners. Panel 2A fails at a load of 188 kN/m, which is essentially the same as the failure load for panels 1A and 1B. However, the primary cause of failure is delamination of a stiffener from the skin. The initial buckling

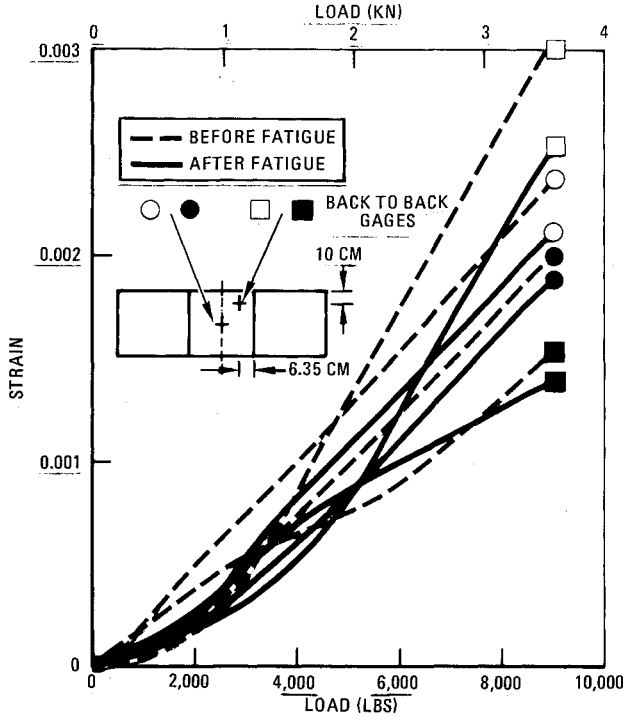

Fig. 4 Strain along tension field direction for panel 1B.

load of this panel is approximately 18 kN/m. Panel 2B loaded in fatigue displays behavior similar to that of panel 1B. The delaminations between stiffeners and the skin, however, are slightly more pronounced. The initial buckling for this panel occurs at a load of 4.68 kN/m which is considerably lower than for panel 2A. The much lower buckling load cannot be explained other than by speculating that some residual stresses are built into the panel during the assembly of the test fixture. The buckling load of panel 2B is found to be lower (2.34 kN/m) after fatigue. This reduction in buckling load due to fatigue is similar to the behavior of panel 1B.

Panels 3A and 3B have hat stiffeners and are shorter in length than the other panels. Panel 3A, which is loaded statically, fails at a load of 298 kN/m. The failure is due primarily to delamination of a stiffener from the skin. A loud noise is emitted. Failure of the web results immediately following the delamination. The panel buckles at a load of 42 kN/m, which is approximately 15% of the ultimate failure load. The center bay of the panel buckles in two half waves because of the aspect ratio of the web. The average failure strain for this panel is 0.006.

Panel 3B is subjected to fatigue loading. The maximum load amplitude during fatigue loading is 187.2 kN/m. The panel develops a visible delamination between a stiffener and the skin after about 2000 cycles in the lower corner of the diagonal tension fields. A delamination in the upper corner of the diagonal tension fields appears soon after. The specimen after 250,000 cycles of fatigue load is shown in Fig. 5. The crack in the center bay starts on the left side after 50,000 cycles and increases in size steadily. The panel is assumed to have failed, and no residual strength test is conducted. Examination of Fig. 5 reveals the crack in the center bay extends through (under) the stiffeners on diagonally opposite corners. Delamination between the stiffener and the skin is clearly visible during fatigue after only 2000 cycles, so the failure of the skin can be termed as secondary failure. Thus, the skin failure observed during fatigue cannot be considered as a typical primary failure mode for these panels.

Correlation of Experimental Data with Analytical Results

Test panels 1A, 1B, 2A, and 2B have two predominant failure modes, "compression failure" and "stiffener-web

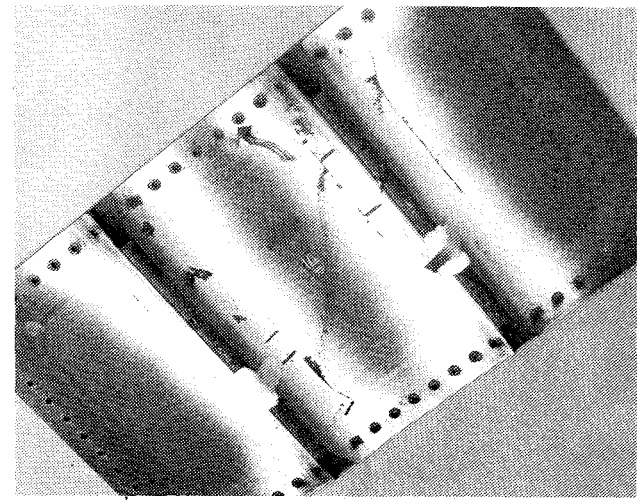

Fig. 5 Specimen 3B after 250,000 cycles of constant amplitude fatigue.

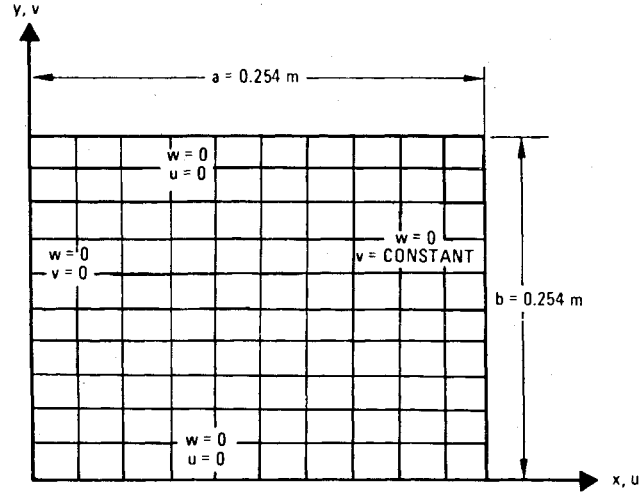

Fig. 6 NASTRAN model for the skin of the test specimen center bay.

delamination," which are observed experimentally. The compression failure is due to high compressive stresses caused by bending of the web resulting from the buckles, and the stiffener-web delamination is due to delamination of a stiffener from the skin. Both of these failure modes are different from those observed for metal shear webs. In metal shear beams, the primary failure mode is due to web rupture or due to formation of permanent buckles in the web. The failure load based upon metal "tension field theory"[4] of these test panels due to web rupture is about two times the experimentally observed ultimate failure load. Because the observed failure modes for composite panels cannot be predicted by the use of conventional tension field theory, a more refined analysis is required. The postbuckling behavior of shear panels involves large displacements, so the equations governing the behavior of such panels are nonlinear. The nonlinearity introduced by the large deflections, generally referred to as "geometric nonlinearity," makes it impossible to obtain closed-form solutions. Another form of nonlinearity, generally referred to as material nonlinearity, is introduced when the stresses in the panel are higher than the proportional limit. In the present paper, an attempt is made to include geometric nonlinearity in obtaining the analytical prediction of the test panel failure loads. The results of this effort are presented subsequently.

Test panels 1A, 1B, 2A, and 2B are essentially identical except for the stiffener shape. The stiffeners are quite stiff to

force failures of the skin. In order to model the failure of the skin in the tension field corner, as well as to study the behavior near the edges of the skin-stiffener interface, a plate representing the skin of the test panel and having the dimensions of the center bay is analyzed. The plate dimensions are selected by ignoring the builtup areas. The plate is then analyzed through the use of the geometric nonlinear analysis feature of the NASTRAN computer code (MSC version).[9] The analytical model and the boundary conditions used are shown in Fig. 6. The boundary conditions used along the plate edges are essentially simple support. The plate is modeled using 100 CQUAD4 isoparametric elements, which include bending and anisotropy. However, the effect of transverse shear is neglected. The analysis is performed in several load increments by using the restart capability.

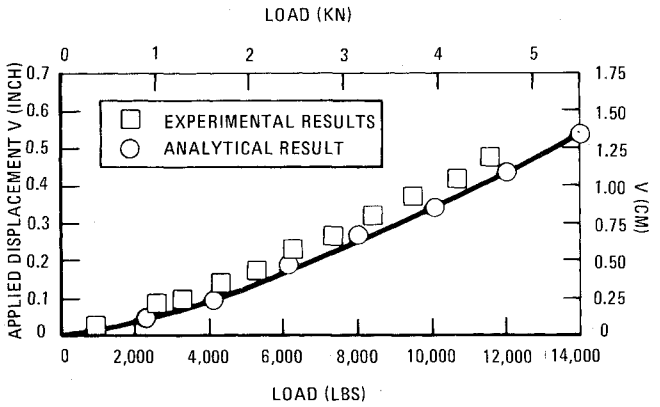

Fig. 7 Analytical and experimental results for applied load and displacements.

Analytical and experimental results for different aspects of panel behavior as well as some interesting analytical observations are presented in Figs. 7-12. The relationship between the applied displacement along the edge vs total applied load is presented in Fig. 7. This relationship is not linear, as expected. The experimental points are obtained by extrapolating the displacements to correspond to the total length of the chords. The analytical displacements are extrapolated linearly to correspond to the width of the test specimen. The total analytical load is the summation of load on all the nodes along one side of the plate. The experimental and analytical correlation of the results in Fig. 7 is quite good.

The normal displacement contours obtained analytically are presented in Fig. 8 for an average applied load of 175 kN/m. The deflection contours exhibit very similar behavior to that observed experimentally by Moire fringes (see Fig. 3). The experimentally measured deflections are also shown at different locations on Fig. 8 for an average applied shear of 163 kN/m. The correlation between measured and analytically predicted values is quite good.

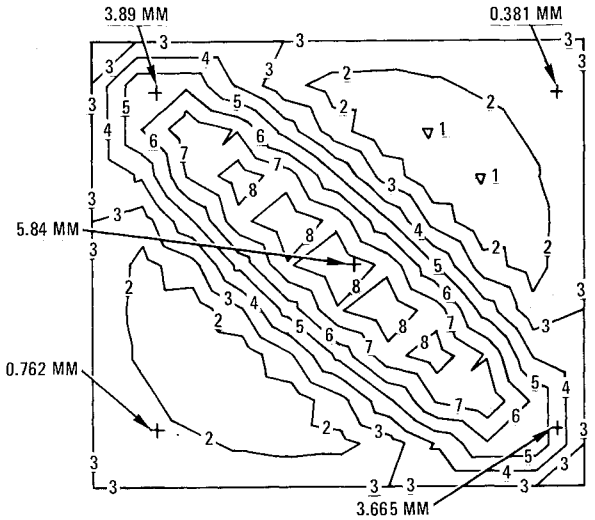

SYMBOL	DISPLACEMENT (MM)
1	2.54
2	1.27
3	0.00
4	-1.27
5	-2.54
6	-3.81
7	-5.08
8	-6.35
9	-7.62

LOAD LEVEL N_{xy} = 175 KN/M
MAXIMUM DEFLECTION = 6.825 MM
+ EXPERIMENTALLY MEASURED VALUES AT (N_{xy} = 163 KN/M)

Fig. 8 Predicted normal displacement contours.

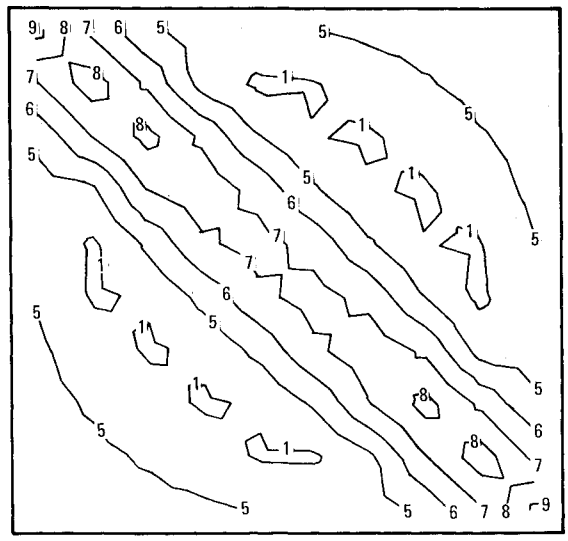

SYMBOL	VALUE (M Pa)
1	172
2	345
3	517
4	689
5	0
6	-172
7	-345
8	-517
9	-689

LOAD LEVEL = 175 KN/M

Fig. 9 Predicted maximum diagonal stresses due to bending.

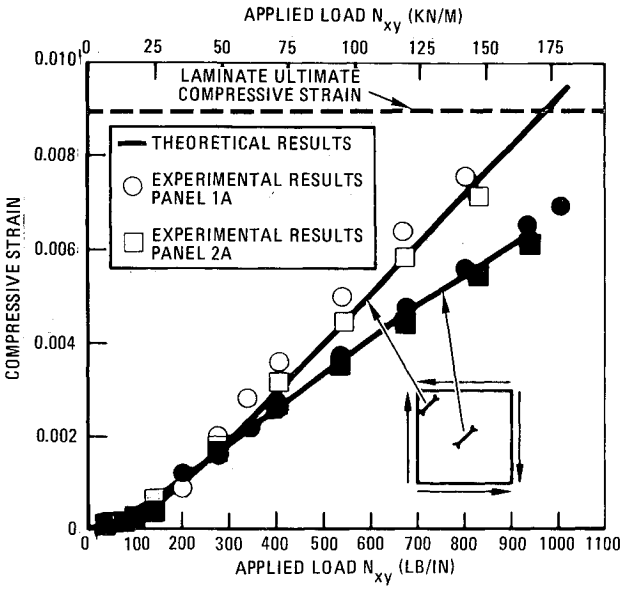

Fig. 10 Experimental and analytical maximum diagonal strains.

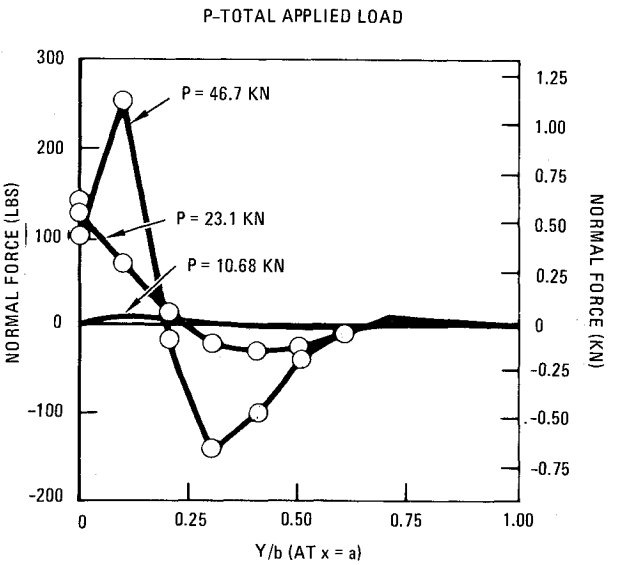

Fig. 12 Normal constraint force due to the postbuckling deflection of the plate.

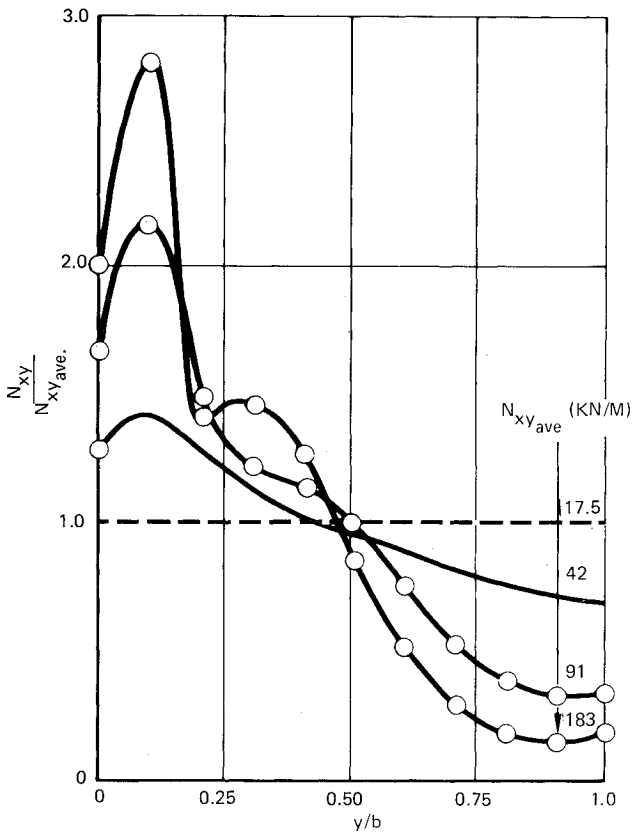

Fig. 11 Variation of applied shear along the plate edge.

The maximum diagonal stresses due to out-of-plane web bending obtained from NASTRAN are presented in the form of a contour plot in Fig. 9. There are concentrations of stress in the top left and lower right corners. A failure in the top left corner of panel 1A is observed experimentally as shown in Fig. 3. Similarly, high concentrations of strains are recorded in these corners for panels 1B, 2A, and 2B. The strain values obtained by NASTRAN are plotted as a function of applied average shear load in Fig. 10 at two different locations. The circles and squares represent experimental data for panels 1A and 2A, respectively. The open symbols represent values in the corner, and solid symbols represent values in the center of the plate.

An excellent correlation between the experimental results and analytical predictions is noted. The ultimate compressive strain for the web laminate is about 0.009 as shown in Fig. 10. The ultimate failure load corresponding to this strain is 166.3 kN/m of shear whereas a failure load of 177 kN/m is observed for panel 1A. The experimental failure load thus corresponds closely to the analytically obtained failure load. However, the use of a compression allowable strain is not totally justified, because the laminate failure occurs because of compressive stresses introduced due to a combined action of compression and bending forces in the plate. The material allowable strain due to combined compression and bending is not easy to obtain, so use of an allowable strain in which compression is assumed to occur throughout the thickness may be satisfactory. The results in Fig. 10 are support to the claim that large deflection theory can be used to predict the behavior of shear plates quite accurately.

In the mathematical model presented in Fig. 6 the load is introduced by applying a constant displacement along the edge $x=a$. The average applied shear is calculated by averaging the loads at all the node points along this edge. The variation of load normalized with respect to the average load along the edge $x=a$ is presented in Fig. 11 for various values of average load. The load is almost uniform at small values of average load, but a significant concentration is introduced near the corner as the average load is increased. Thus, the assumption of constant shear along the edge in an analysis may lead to considerable error in predicted behavior as against observed behavior. The experimental setup that was used in this program essentially introduces constant displacement along the edge, as is assumed in the analysis.

In an attempt to shed light on the delaminations observed in between the stiffeners and the skin, the normal forces introduced due to the large deflections of the plate are plotted in Fig. 12 along the edges $x=a$ as a function of increasing total applied load. The normal forces increase significantly near the corner as the load is increased. These normal forces act in between the stiffener-web interface to cause separation of stiffener from the web.

In the foregoing discussion, the stiffener is not included in the analysis, and also the edges are allowed to rotate. Because the stiffeners offer rotational constraint, additional normal forces at the stiffener-skin interface are introduced. Interlaminar shear also may be significant at these locations, but is not included in the analysis presented here. Therefore, no quantitative evaluation of failure load resulting in delamination of the stiffener from the skin is made in this

paper. The results presented in Fig. 12 show a concentration of normal forces, thus indicating a trend toward possible location of a delamination.

Summary and Conclusion

The results of an experimental and analytical study to evaluate the postbuckling behavior of composite stiffened shear panels are presented in this paper. The panels are designed to have significant postbuckling strength with the ultimate failure load to initial buckling load ratio of at least five to one (ratios up to 10 are achieved). Six stiffened panels are designed and fabricated with each panel being different either in construction or in loading, i.e., no tests are replicated. The conclusions made in this paper are based upon the result of a single test, so a further verification of these findings is recommended.

The fabrication of panels is accomplished by using removable rubber mandrels to form cocured stiffeners. Two different stiffener shapes, hat and I, were used. The fabrication of hat-stiffened panels is easier and less expensive than the fabrication of I-stiffened panels.

Two predominant failure modes are observed. The first mode of failure, "compression failure" is due to high compressive stresses introduced by the buckles in the tension field corners. These stresses in the corners are considerably higher than the stresses in the center of the panels. The second mode of failure, "stiffener-web delamination," is due to delamination of the stiffeners from the skin. The delaminations are easily visible for panels during fatigue, but for panels under static load the delamination occurs with a loud popping noise.

The fatigue loading on the panels introduces delaminations near the diagonal tension corners in between the interface of the skin and the stiffeners for all the panels loaded under fatigue. However, these delaminations become stable after about 50,000 cycles and do not grow in size. No loss in the strength of fatigue panels was found, even though these panels exhibited significant stiffener-web delaminations. The panels containing hat stiffeners and I-section stiffeners fail at approximately the same load. This result, however, should not be interpreted as being generally the case because the stiffeners are quite stiff.

The failure modes observed during testing (compression failure and stiffener-web delamination) are not predictable through the use of conventional "tension field theory" developed for metal shear webs. The geometric nonlinear analysis option of the NASTRAN computer program is used to predict the postbuckling behavior of the test panels. The NASTRAN analysis is a good prediction of the postbuckling response as well as the failure load for the compression failure mode in the diagonal tension corners. The analytical and experimental correlations for load vs applied vertical displacement, as well as for load vs resulting out-of-plane displacements and in-plane stresses, are very good. As the applied displacement along the plate edge is increased, the resulting load distribution along the plate edge becomes quite nonuniform. Significantly higher loads are calculated near the diagonal tension end than near the other end.

A large concentration of normal forces near the diagonal tension corners results due to constraint against normal displacements. The stiffener-web delaminations were observed in these corners. No quantitative prediction of the failure load for this mode of failure is made due to the limitations of the model. A more extensive model needs to be used to account for the effect of transverse shear forces between the interface of the stiffener and the skin, as well as to account for the rotational constraint provided by the stiffener.

Acknowledgments

The work reported herein was supported by Northrop's Independent Research and Development Program. Contributions of V. C. Frost and L. Bernhardt are greatly appreciated.

References

[1] Kaminski, B. E. and Ashton, J. E., "Diagonal Tension Behavior of Boron-Epoxy Shear Panels," *Journal of Composite Materials,* Vol. 5, Oct. 1971, pp. 553-558.

[2] Bhatia, N. M., "Postbuckling Fatigue Behavior of Advanced Composite Shear Panels," *Proceedings of the Army Symposium on Solid Mechanics, 1976 - Composite Materials, The Influence of Failure on Design,* Army Materials and Mechanics Research Center, Watertown, Mass., Rept. MS 76-3, 1976.

[3] Wagner, H., "Flat Sheet Metal Girders with Very Thin Metal Web," Parts I, II and III, NACA TM 604, 605, and 606, 1931.

[4] Kuhn, P., Peterson, M. P., and Levin, L. R., "Summary of Diagonal Tension, Parts I and II," NACA TM 2661 and 2662, May 1952.

[5] Tsongas, A. G. and Ratay, R. T., "Investigation of Diagonal-Tension Beams with Very Thin Stiffened Webs," NASA CR 101854, July 1969.

[6] Darevics, V. M. and Hoy, J. D., "SST Technology Follow-On Program, Phase I, Intermediate Shear Beam Analyses," Federal Aviation Agency, Washington, D. C., Rept. FAA-SS-72-11, May 1972.

[7] Almoroth, B. O., Brogan, F. A., and Stanley, G. M., "Structural Analysis of General Shells, Vol. II, User Instruction for STAGSC," Lockheed Missiles and Space Company, Inc., Sunnyvale, Calif., Rept. LMSCD502277, Dec. 1975.

[8] DeSalvo, G. J. and Swanson, J. A., "ANSYS Engineering Analysis System User's Manual," Swanson Analysis Systems Inc., Elizabeth, Penna., March 1975.

[9] McCormick W. C., ed., "MSC/NASTRAN User's Manual," MacNeal-Schwendler Corp., Los Angeles, Calif., May 1976.

[10] Hayes, R. D., "Flightworthy Graphite Fiber Reinforced Composite Aircraft Primary Structural Assemblies," Air Force Materials Laboratory, Dayton, Ohio, Vol. I, AFML-TR-71-276, April 1972.

[11] Rich, M. J., "Low Cost Composite Airframe Structures," Third Conference on Fibrous Composites in Flight Vehicle Design, 1975, NASA TM X-3337, 1975.